# Optimization of Multi-UAV-BS Aided Millimeter-Wave Massive MIMO Networks

Lipeng Zhu[†], Jun Zhang[†‡], Zhenyu Xiao[†], and Robert Schober[§]
[†]School of Electronic and Information Engineering, Beihang University, Beijing, 100083, China.
[‡]Advanced Research Institute of Multidisciplinary Science, Beijing Institute of Technology, Beijing, 100081, China.
[§]Institute for Digital Communications, Friedrich-Alexander University of Erlangen-Nuremberg, Erlangen 91054, Germany.
Email: zhulipeng@buaa.edu.cn, buaazhangjun@vip.sina.com, xiaozy@buaa.edu.cn, robert.schober@fau.de

***Abstract*—In this paper, we investigate millimeter-wave (mmWave) massive multiple-input multiple-output (MIMO) networks with multiple unmanned aerial vehicle (UAV) mounted base stations (BSs). Uniform planar arrays are equipped at the UAV-BSs to perform hybrid analog-digital beamforming (BF) for compensation of the high path loss of mmWave channels and for mitigation of intra-cell and/or inter-cell interference. We jointly optimize the UAV-BS positioning, user assignment, and hybrid BF for maximization of the achievable sum rate (ASR) of the users, subject to a minimum rate constraint for each user. A sub-optimal solution for the resulting high-dimensional and non-convex problem is developed by exploiting alternating optimization, successive convex optimization, and combinatorial optimization. Our simulation results verify the convergence of the proposed algorithm and demonstrate significant performance gains compared to two benchmark schemes in terms of the ASR.**

***Index Terms*—UAV communication, millimeter-wave, positioning, user assignment, hybrid beamforming.**

## I. Introduction

Unmanned aerial vehicle (UAV) aided communication has been considered as one of the key technologies for beyond fifth-generation (B5G) and sixth-generation (6G) mobile networks [1]. Due to their flexible deployment and low cost, UAVs can serve as aerial base stations (BSs) to enlarge the coverage of the terrestrial networks and to improve the quality of service (QoS) of the ground users. In the past few years, significant research efforts have been dedicated to the optimization of UAV-BS aided wireless communication systems, including UAV placement [2], [3], trajectory design [4], [5], and resource allocation [6].

In general, a single UAV-BS can provide only limited user coverage and access, while a cooperative network of multiple UAV-BSs can efficiently enlarge the coverage region and increase the number of served users. Thus, we consider a network of multiple UAV-BSs in this paper. Because of the heavy traffic in the microwave frequency bands below 6 GHz, meeting the high-data-rate requirements of future mobile communication systems has become very challenging. To address this problem, millimeter-wave (mmWave) communication with its large available bandwidth is a promising technology for application in UAV systems. Besides, UAVs usually suffer severe interference from other aerial platforms because the corresponding channels follow the free-space attenuation model [1], [4]. The sparsity of the mmWave channels and the directionality of mmWave beams make it possible to significantly reduce the interference in UAV communications. On the other hand, the performance of mmWave communication systems is highly depended on the existence of line of sight (LoS) links because the non-LoS (NLoS) paths are highly attenuated. For UAV platforms operating at higher altitudes, it is easier to establish a LoS link, which is ideal for mmWave communication.

Enabling UAV cellular with mmWave systems was first proposed in [7], where the potentials, challenges, and preliminary solutions for UAV-mmWave communication were discussed. Recently, UAV-mmWave communication has attracted significant attention. The channel characteristics, channel acquisition, and communication design for UAV-mmWave networks were studied in [8]. The authors of [9] proposed a beam tracking strategy for UAV systems employing joint beam training and angular velocity estimation. Besides, beam tracking schemes for UAV-satellite and UAV-to-UAV communication systems were investigated in [10] and [11], respectively. In [12], a novel spectrum management strategy for UAV-assisted mmWave cellular networks was proposed. The joint design of positioning and analog beamforming (BF) was investigated for a single UAV BS and for a UAV relay in [13] and [14], respectively.

Different from the works above, we consider a mmWave multiple-input multiple-output (MIMO) network employing multiple UAV-BSs to serve multiple ground users, which can be potentially used in the hot-spot and/or remote areas to provide large-bandwidth communication service. Hybrid analog-digital BF techniques are utilized at the UAV-BSs to compensate for the high path loss of mmWave channels and to mitigate intra-cell and/or inter-cell interference. To the best of our knowledge, this is the first work that investigates the deployment and optimization of multiple UAV-BSs employing hybrid BF structures in the mmWave frequency bands. Specifically, we jointly optimize the UAV-BS positioning, user assignment, and hybrid BF for maximization of the achievable sum rate (ASR) of the users, subject to a minimum rate constraint for each user. The resulting problem is highly non-convex and involves high-dimensional variable matrices and combinatorial programming variables, where the positions of UAV-BSs impact both the amplitudes and the directivities of the mmWave channels between the UAVs and users. The proposed two-step solution novelly decouples the directional BF portion from the original problem. We first develop an iterative algorithm to optimize the positions of the UAV-BSs and the user assignment under the assumption of ideal BF. Then, for the given positions of the UAV-BSs and the given user assignments, we alternately optimize the analog BF matrices and the digital BF matrices to maximize the ASR of the users. Our simulation results verify the convergence of the proposed algorithms and reveal significant performance gains compared to two benchmark schemes in terms of the ASR. Furthermore, the proposed hybrid BF scheme is shown

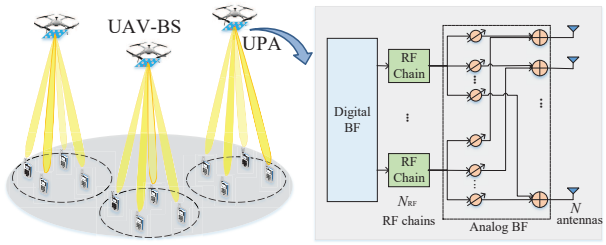


Fig. 1. Illustration of the considered multi-UAV-BS aided downlink mmWave massive MIMO network.

to closely approach the performance of fully digital BF.

## II. System Model and Problem Formulation

As shown in Fig. 1, we consider a downlink mmWave network where $M$ UAV-BSs are deployed to serve $K$ single-antenna users. The UAV-BSs are equipped with uniform planar arrays (UPAs) employing $N = N_x \times N_y$ antennas fully connected with $N_{\rm RF}$ radio frequency (RF) chains via $N_{\rm RF}N$ phase shifters [15]. The sets of UAV-BSs and users are denoted as $\mathcal{M}$ and $\mathcal{K}$, respectively. In this paper, we assume $K = MN_{\rm RF}$. The user set served by UAV-BS $m$ is denoted by $\mathcal{K}_m$, where we assume $|\mathcal{K}_m| = N_{\rm RF}$ and $\bigcup_{m\in\mathcal{M}} \mathcal{K}_m = \mathcal{K}$[1]. The horizontal coordinates of user $k$ are given by $\mathbf{u}_k = [x_k, y_k] \in \mathbb{R}^{2\times 1}$. We assume that the altitudes of the UAV-BSs are fixed to $H$, and the horizontal coordinates of UAV-BS $m$ are denoted by $\mathbf{v}_m = [X_m, Y_m] \in \mathbb{R}^{2\times 1}$.

At each user $k \in \mathcal{K}_m$, the received signal is given by

$$\bar{y}_k = \mathbf{h}_{m,k}^{\rm H}\mathbf{A}_m\mathbf{D}_m\mathbf{s}_m + \sum_{j\neq m} \mathbf{h}_{j,k}^{\rm H}\mathbf{A}_j\mathbf{D}_j\mathbf{s}_j + n_k, \tag{1}$$

where $\mathbf{h}_{m,k} \in \mathbb{C}^{N\times 1}$ is the channel vector between UAV-BS $m$ and user $k$. $(\cdot)^{\rm H}$ denotes the conjugate transpose. $\mathbf{A}_m \in \mathbb{C}^{N\times N_{\rm RF}}$ and $\mathbf{D}_m \in \mathbb{C}^{N_{\rm RF}\times N_{\rm RF}}$ are the analog and digital BF matrices of UAV-BS $m$, respectively. $\mathbf{s}_m \sim \mathcal{CN}(\mathbf{0}, \mathbf{I}_{N_{\rm RF}})$ is signal transmitted by UAV-BS $m$, where $\mathcal{CN}(\mathbf{\Gamma}, \mathbf{\Sigma})$ denotes Gaussian distribution with mean $\mathbf{\Gamma}$ and covariance matrix $\mathbf{\Sigma}$, and $\mathbf{I}_{N_{\rm RF}} \in \mathbb{R}^{N_{\rm RF}\times N_{\rm RF}}$ is a unit matrix. Each element of $\mathbf{s}_m$ represents an independent data stream intended for one user, and $n_k \sim \mathcal{CN}(0, \sigma^2)$ is the noise at user $k$.

We assume the UAV-to-user links are LoS and neglect the NLoS components which are typically more than 20 dB weaker than the LoS components in the mmWave band. Hence, the channel vector between UAV-BS $m$ and user $k$ is modeled as [7]–[11]

$$\mathbf{h}_{m,k} = \frac{\beta_0}{(H^2 + \|\mathbf{v}_m - \mathbf{u}_k\|_2^2)^{\alpha/4}}\sqrt{N}\mathbf{a}(\theta_{m,k}, \phi_{m,k}), \tag{2}$$

where $\beta_0 = \frac{c_0}{4\pi f_c}$ denotes the channel gain at reference distance $d_0 = 1$ m, $c_0$ is the constant speed of light, and $f_c$ is the carrier frequency. $\alpha \geq 2$ is the large-scale path loss exponent for mmWave signals. $\theta_{m,k}$ and $\phi_{m,k}$ are respectively the elevation angle of departure (AoD) and the azimuth AoD of the LoS path between UAV-BS $m$ and user $k$ [14]. $\mathbf{a} \in \mathbb{C}^{N\times 1}$ is the UPA steering vector given by $\mathbf{a}(\theta, \phi) = \frac{1}{\sqrt{N}}[e^{j2\pi\frac{d}{\lambda}\cos\theta[(n_x-1)\cos\phi+(n_y-1)\sin\phi]}]^{\rm T}$ with $1 \leq n_x \leq N_x, 1 \leq n_y \leq N_y$, where $d$ is the spacing between adjacent antennas and $\lambda$ is the carrier wavelength. Particularly, for half-wavelength spaced arrays, we have $d = \lambda/2$.

Then, we obtain the signal-to-interference-plus-noise ratio (SINR) of the $n$th user served by UAV-BS $m$ as follows

$$\gamma_{m,n} = \frac{\left|\mathbf{h}_{m,k_{m,n}}^{\rm H}\mathbf{A}_m\mathbf{d}_{m,n}\right|^2}{\sum\limits_{i\neq n}\left|\mathbf{h}_{m,k_{m,n}}^{\rm H}\mathbf{A}_m\mathbf{d}_{m,i}\right|^2 + \sum\limits_{j\neq m}\left\|\mathbf{h}_{j,k_{m,n}}^{\rm H}\mathbf{A}_j\mathbf{D}_j\right\|_2^2 + \sigma^2}, \tag{3}$$

where $k_{m,n}$ is the index of the $n$th user served by UAV-BS $m$ and $\mathbf{D}_m = [\mathbf{d}_{m,1}, \mathbf{d}_{m,2}, \cdots, \mathbf{d}_{m,N_{\rm RF}}]$. As a result, the achievable rate of user $k_{m,n}$ is given by

$$R_{m,n} = \log_2(1 + \gamma_{m,n}). \tag{4}$$

To maximize the ASR of the ground users, we formulate the following problem for joint optimization of the UAV-BS positioning, user assignment, and hybrid BF:

$$\max_{\{\mathbf{v}_m, \mathcal{K}_m, \mathbf{A}_m, \mathbf{D}_m\}} \quad \sum_{m\in\mathcal{M}}\sum_{1\leq n\leq|\mathcal{K}_m|} R_{m,n} \tag{5a}$$

$$\text{s.t.} \quad |\mathcal{K}_m| = N_{\rm RF},\ \forall m, \tag{5b}$$

$$\bigcup_{m\in\mathcal{M}} \mathcal{K}_m = \mathcal{K}, \tag{5c}$$

$$\left|[\mathbf{A}_m]_{i,j}\right| = \frac{1}{\sqrt{N}},\ \forall m,\ i,\ j, \tag{5d}$$

$$\|\mathbf{A}_m\mathbf{D}_m\|_F^2 \leq P,\ \forall m, \tag{5e}$$

$$R_{m,n} \geq r_{m,n},\ \forall m,\ 1 \leq n \leq |\mathcal{K}_m|, \tag{5f}$$

where constraint (5d) is the constant-modulus (CM) constraint on the analog BF matrices. Constraint (5e) ensures that the transmit power of each UAV-BS cannot exceed a maximum value $P$. Constraint (5f) guarantees that the achievable rate of each user is no less than the required rate $r_{m,n}$. Problem (5) is highly non-convex and cannot be directly solved via existing optimization tools. Thus, we develop a sub-optimal solution for (5) in the next section.

## III. Solution of the Problem

In this section, we first optimize the UAV-BS positioning and user assignment under the assumption of ideal BF. Then, given the positions of the UAV-BSs and the user assignment, we propose an alternating optimization algorithm for optimization of the analog and digital BF matrices.

### A. Joint UAV-BS Positioning and User Assignment

Since the high-dimensional and highly coupled BF matrices make Problem (5) intractable, we first assume ideal BF to simplify the original problem. According to antenna theory, the array gain of a user is maximized if and only if the steering vector for the channel between the user and its serving UAV-BS is used for BF. Hence, we define ideal BF as follows.

**Definition 1.** ***(Ideal BF)*** *For ideal BF (which may not be realizable), the full array gains are obtained for the target signals, while all interference is completely eliminated, i.e.,*

$$\begin{cases} \left|\mathbf{h}_{m,k_{m,n}}^{\rm H}\mathbf{A}_m^{\rm id}\mathbf{d}_{m,n}^{\rm id}\right|^2 = \dfrac{\beta_0^2 N p_{m,n}}{\left(H^2 + \left\|\mathbf{v}_m - \mathbf{u}_{k_{m,n}}\right\|_2^2\right)^{\alpha/2}}, \\ \sum\limits_{i\neq n}\left|\mathbf{h}_{m,k_{m,n}}^{\rm H}\mathbf{A}_m^{\rm id}\mathbf{d}_{m,i}^{\rm id}\right|^2 + \sum\limits_{j\neq m}\left\|\mathbf{h}_{j,k_{m,n}}^{\rm H}\mathbf{A}_j^{\rm id}\mathbf{D}_j^{\rm id}\right\|_2^2 = 0, \end{cases} \tag{6}$$

[1]When the users are not equally clustered, a generalized scheme can be obtained by improving the proposed solution and will be discussed in our future work.

*where* $p_{m,n} = \left\|\mathbf{A}_m^{\mathrm{id}}\mathbf{d}_{m,n}^{\mathrm{id}}\right\|_2^2$ *is the signal power for user* $k_{m,n}$. $\mathbf{A}_m^{\mathrm{id}}$ *and* $\mathbf{D}_m^{\mathrm{id}} = [\mathbf{d}_{m,1}^{\mathrm{id}}, \mathbf{d}_{m,2}^{\mathrm{id}}, \cdots, \mathbf{d}_{m,|\mathcal{K}_m|}^{\mathrm{id}}]$ *are the ideal analog and digital BF matrices, respectively.*

Substituting (6) into (3) and (4), we obtain an (non-achievable) upper bound for the achievable rate of user $k_{m,n}$ as follows

$$\bar{R}_{m,n} = \log_2\left(1 + \frac{\beta_0^2 N p_{m,n}}{\left(H^2 + \left\|\mathbf{v}_m - \mathbf{u}_{k_{m,n}}\right\|_2^2\right)^{\alpha/2}\sigma^2}\right). \quad (7)$$

Next, we optimize the UAV-BS positioning and user assignment for maximization of the upper bound in (7). Let $\mathbf{p}_m = [p_{m,1}, p_{m,2}, \cdots, p_{m,N_{\mathrm{RF}}}]^{\mathrm{T}}$ denote the power allocation vector of UAV-BS $m$. Problem (5) is simplified as follows

$$\max_{\{\mathbf{v}_m, \mathcal{K}_m, \mathbf{p}_m\}} \quad \sum_{m\in\mathcal{M}}\sum_{1\le n\le|\mathcal{K}_m|} \bar{R}_{m,n} \quad (8a)$$

$$\text{s.t.} \quad \text{(5b), (5c)} \quad (8b)$$

$$\bar{R}_{m,n} \ge r_{m,n},\ \forall m,\ n. \quad (8c)$$

Problem (8) is still a combinatorial programming problem and involves highly coupled variables. We propose an efficient iterative algorithm for solving this non-convex problem. First, the users are clustered into $M$ groups based on their horizontal coordinates by employing the K-means algorithm, where the summation of the Euclidean distances from the cluster centers to their assigned users is minimized. The initial horizonal positions of the UAV-BSs are at the cluster centers, while the initial user assignment corresponds to the users in the cluster. Then, we start an iterative process as follows.

*1) Power Allocation:* For given $\{\mathbf{v}_m^{(t-1)}, \mathcal{K}_m^{(t-1)}\}$ obtained in the $(t-1)$th iteration, the power allocation vectors of different UAV-BSs are mutually independent. For UAV-BS $m$, we solve the following problem:

$$\max_{\mathbf{p}_m} \quad \sum_{1\le n\le|\mathcal{K}_m|} \bar{R}_{m,n} \quad (9a)$$

$$\text{s.t.} \quad \bar{R}_{m,n} \ge r_{m,n},\ \forall n. \quad (9b)$$

Problem (9) is a standard concave problem with respect to $\mathbf{p}_m$. It can be solved by utilizing the water-filling algorithm. The optimal solution for power allocation in closed form is given by

$$p_{m,n}^{(t)} = \max\left\{\lambda_m - \frac{1}{g_{m,n}}, \frac{2^{r_{m,n}}-1}{g_{m,n}}\right\}, \quad (10)$$

where $g_{m,n} = \frac{\beta_0^2 N}{(H^2+\left\|\mathbf{v}_m^{(t-1)}-\mathbf{u}_{k_{m,n}}\right\|_2^2)^{\alpha/2}\sigma^2}$ and $\lambda_m$ is chosen to satisfy $\sum_{1\le n\le|\mathcal{K}_m|} p_{m,n}^{(t)} = P$.

*2) UAV-BS Positioning:* For given $\{\mathbf{v}_m^{(t-1)}, \mathcal{K}_m^{(t-1)}, \mathbf{p}_m^{(t)}\}$, the positions of the UAV-BSs are optimized by solving the following problem:

$$\max_{\{\mathbf{v}_m\}} \quad \sum_{m\in\mathcal{M}}\sum_{1\le n\le|\mathcal{K}_m|} \bar{R}_{m,n} \quad (11a)$$

$$\text{s.t.} \quad \bar{R}_{m,n} \ge r_{m,n},\ \forall m,\ n. \quad (11b)$$

Problem (11) is not convex due to the non-convex form of $\bar{R}_{m,n}$. To tackle this problem, we exploit successive convex optimization. The achievable rate in (11) is rewritten as $\bar{R}_{m,n} = \log_2 f_{m,n} + \hat{R}_{m,n}$ where $f_{m,n} = \frac{(H^2+\|\mathbf{v}_m-\mathbf{u}_{k_{m,n}}\|_2^2)^{\alpha/2}+g_0 p_{m,n}}{(H^2+\|\mathbf{v}_m^{(t-1)}-\mathbf{u}_{k_{m,n}}\|_2^2)^{\alpha/2}}$, $\hat{R}_{m,n} = -\frac{\alpha}{2}\log_2\frac{H^2+\left\|\mathbf{v}_m-\mathbf{u}_{k_{m,n}}\right\|_2^2}{H^2+\left\|\mathbf{v}_m^{(t-1)}-\mathbf{u}_{k_{m,n}}\right\|_2^2}$, and $g_0 = \frac{\beta_0^2 N}{\sigma^2}$. As can be observed, both $f_{m,n}$ and $\hat{R}_{m,n}$ are convex with respect to $\left\|\mathbf{v}_m - \mathbf{u}_{k_{m,n}}\right\|_2^2$. Furthermore, $\left\|\mathbf{v}_m - \mathbf{u}_{k_{m,n}}\right\|_2^2$ is convex with respect to $\mathbf{v}_m$. Thus, $f_{m,n}$ and $\hat{R}_{m,n}$ can be lower-bounded by their first-order Taylor expansions at point $\mathbf{v}_m^{(t-1)}$, i.e.,

$$f_{m,n} \ge A_{m,n}(\mathbf{v}_m^{(t-1)} - \mathbf{u}_{k_{m,n}})^{\mathrm{T}}(\mathbf{v}_m - \mathbf{v}_m^{(t-1)}) + B_{m,n} \triangleq \Gamma_{m,n}, \quad (12)$$

$$\hat{R}_{m,n} \ge C_{m,n}(\mathbf{v}_m^{(t-1)} - \mathbf{u}_{k_{m,n}})^{\mathrm{T}}(\mathbf{v}_m - \mathbf{v}_m^{(t-1)}) \triangleq \Upsilon_{m,n}, \quad (13)$$

where $A_{m,n} = \alpha(H^2 + \|\mathbf{v}_m^{(t-1)} - \mathbf{u}_{k_{m,n}}\|_2^2)^{-1}$, $B_{m,n} = 1 + g_0 p_{m,n}^{(t)}(H^2 + \|\mathbf{v}_m^{(t-1)} - \mathbf{u}_{k_{m,n}}\|_2^2)^{\alpha/2}$, and $C_{m,n} = -\alpha(H^2 + \|\mathbf{v}_m^{(t-1)} - \mathbf{u}_{k_{m,n}}\|_2^2)^{-1}\ln 2$. Then, Problem (11) is relaxed as follows

$$\max_{\{\mathbf{v}_m\}} \quad \sum_{m\in\mathcal{M}}\sum_{1\le n\le|\mathcal{K}_m|} \log_2\Gamma_{m,n} + \Upsilon_{m,n} \quad (14a)$$

$$\text{s.t.} \quad \log_2(\Gamma_{m,n}) + \Upsilon_{m,n} \ge r_{m,n},\ \forall m,\ n, \quad (14b)$$

$$\left\|\mathbf{v}_m - \mathbf{v}_m^{(t-1)}\right\|_2^2 \le d^{(t)},\ \forall m. \quad (14c)$$

Note that inequalities (12) and (13) are only valid in a small neighborhood of point $\mathbf{v}_m^{(t-1)}$. Hence, constraint (14c) is introduced, where parameter $d^{(t)}$ represents a radius of a spherical neighborhood and gradually decreases during the iterations to guarantee convergence. One possible choice is $d^{(t)} = d^{(t-1)}/\kappa_1$, where $\kappa_1 > 1$ is the step size for the reduction of the radius. Problem (14) is convex and the optimal solution $\mathbf{v}_m^{(t)}$ can be obtained by using convex optimization tools such as CVX.

*3) User Assignment:* For given $\{\mathbf{v}_m^{(t)}, \mathcal{K}_m^{(t-1)}, \mathbf{p}_m^{(t)}\}$, the user assignment variables are optimized by solving the following problem:

$$\max_{\{\mathcal{K}_m\}} \quad \sum_{m\in\mathcal{M}}\sum_{1\le n\le|\mathcal{K}_m|} \bar{R}_{m,n} \quad (15a)$$

$$\text{s.t.} \quad \text{(5b), (5c)} \quad (15b)$$

$$\bar{R}_{m,n} \ge r_{m,n},\ \forall m,\ n. \quad (15c)$$

Problem (15) is a combinatorial programming problem. We define a swap matching operation $\varphi_{m,n}^{j,q}$ $(m \ne j)$ where user $k_{m,n}$ and user $k_{j,q}$ switch their serving UAV-BSs while the other users' assignment remain unchanged. If a swap matching operation $\varphi_{m,n}^{j,q}$ increases the objective function (15a) for given $\{\mathbf{v}_m^{(t)}, \mathbf{p}_m^{(t)}\}$ and satisfies constraint (15c), we call $\varphi_{m,n}^{j,q}$ a valid swap, and the corresponding user assignment is changed, i.e.,

$$\mathcal{K}_m(n) \rightleftharpoons \mathcal{K}_j(q),\ \text{if } \varphi_{m,n}^{j,q} \text{ is a valid swap},\ \forall m \ne j. \quad (16)$$

If all swap matching operations have been considered but no valid swap was found, a sub-optimal solution of Problem (15) is obtained given by $\mathcal{K}_m^{(t)}$. The overall algorithm for solving Problem (8) is summarized in Algorithm 1.

### *B. Hybrid BF Design*

After obtaining the solution for the UAV-BS positioning and user assignment, we optimize the hybrid BF matrices to approach ideal BF. For given $\{\mathbf{v}_m, \mathcal{K}_m\}$, Problem (5) simplifies as follows

$$\max_{\{\mathbf{A}_m, \mathbf{D}_m\}} \quad \sum_{m\in\mathcal{M}}\sum_{1\le n\le|\mathcal{K}_m|} R_{m,n} \quad (17a)$$

$$\text{s.t.} \quad \text{(5d), (5e), (5f).} \quad (17b)$$

**Algorithm 1:** Joint UAV-BS positioning and user assignment

1: Initialize $\{\mathbf{v}_m^{(0)}, \mathcal{K}_m^{(0)}\}$ using K-means algorithm. Let $t = 1$.
2: **repeat**
3: Update $\{\mathbf{p}_m^{(t)}\}$ according to (10) for given $\{\mathbf{v}_m^{(t-1)}, \mathcal{K}_m^{(t-1)}\}$.
4: Update $\{\mathbf{v}_m^{(t)}\}$ by solving (14) for given $\{\mathbf{v}_m^{(t-1)}, \mathcal{K}_m^{(t-1)}, \mathbf{p}_m^{(t)}\}$.
5: Update $\{\mathcal{K}_m^{(t)}\}$ according to (16) for given $\{\mathbf{v}_m^{(t)}, \mathcal{K}_m^{(t-1)}, \mathbf{p}_m^{(t)}\}$.
6: Update $t \leftarrow t + 1$.
7: **until** Increase of the objective value is below a threshold $\epsilon_1$

In Problem (17), the analog and digital BF matrices are highly coupled, and the CM constraint on the analog BF matrices in (5d) is highly non-convex. These two aspects pose the main challenges for solving Problem (17). To address this issue, we propose an efficient algorithm which alternately optimizes the analog and digital BF matrices. First, we initialize each column of the analog BF matrices with the steering vector corresponding to the served user and initialize the digital BF matrices as diagonal matrices, i.e.,

$$[\mathbf{A}_m^{(0)}]_{:,n} = \mathbf{a}\left(\theta_{m,k_{m,n}}, \phi_{m,k_{m,n}}\right), \ \forall m, \ n, \\ \mathbf{D}_m^{(0)} = \frac{\sqrt{P}\mathbf{I}_{N_{\mathrm{RF}}}}{\|\mathbf{A}_m\|_F}, \ \forall m. \tag{18}$$

Then, we start an iterative process as follows.

*1) Analog BF:* For given $\{\mathbf{A}_m^{(t-1)}, \mathbf{D}_m^{(t-1)}\}$ obtained in the $(t-1)$th iteration, we optimize each column of the analog BF matrices in a successive manner. For the $n$th column of $\mathbf{A}_m$, i.e., $\mathbf{a}_{m,n}$, we formulate the following problem:

$$\max_{\mathbf{a}_{m,n}} \quad \left|\mathbf{h}_{m,k_{m,n}}^{\mathrm{H}} \bar{\mathbf{A}}_m \mathbf{d}_{m,n}^{(t-1)}\right| \tag{19a}$$

$$\text{s.t.} \quad \left|\mathbf{h}_{m,k_{m,i}}^{\mathrm{H}} \bar{\mathbf{A}}_m \mathbf{d}_{m,n}^{(t-1)}\right| \le \eta_{m,n,m,i}^{(t)}, \ \forall i \ne n, \tag{19b}$$

$$\left|\mathbf{h}_{m,k_{j,q}}^{\mathrm{H}} \bar{\mathbf{A}}_m \mathbf{d}_{m,n}^{(t-1)}\right| \le \eta_{m,n,j,q}^{(t)}, \ \forall j \ne m, \ \forall q, \tag{19c}$$

$$\left|[\mathbf{a}_{m,n}]_i\right| \le \frac{1}{\sqrt{N}}, \ \forall i, \tag{19d}$$

where $\bar{\mathbf{A}}_m = [\mathbf{a}_{m,1}^{(t)}, \cdots, \mathbf{a}_{m,n-1}^{(t)}, \mathbf{a}_{m,n}, \mathbf{a}_{m,n+1}^{(t-1)}, \cdots, \mathbf{a}_{m,N_{\mathrm{RF}}}^{(t-1)}]$. The objective function in (19a) is designed to maximize the effective channel gain of the $n$th user served by UAV-BS $m$. Constraints (19b) and (19c) limit the intra-cell and inter-cell interference, respectively. Parameter $\eta_{m,n,j,q}^{(t)}$ is an upper bound for the interference at user $k_{j,q}$ caused by the signal intended for user $k_{m,n}$, which gradually decreases in the course of the iterations. One possible choice is $\eta_{m,n,j,q}^{(t)} = \left|\mathbf{h}_{m,k_{j,q}}^{\mathrm{H}} \mathbf{A}_m^{(t-1)} \mathbf{d}_{m,n}^{(t-1)}\right| / \kappa_2$ where $\kappa_2 > 1$ is the step size for the reduction of the interference. The CM constraint for the analog BF matrices is relaxed to the convex constraint shown in (19d). In fact, this relaxation has little impact on the performance of the achievable rate as shown in the following theorem.

**Theorem 1.** *There always exists an optimal solution of Problem* (19)*, where at most* $r = \mathrm{rank}(\tilde{\mathbf{H}}_{m,n})$ *elements do not satisfy the CM constraint with* $\tilde{\mathbf{H}}_{m,n} = [\mathbf{h}_{j,q}, (j,q) \in \mathcal{J}_{m,n}]$ *and* $\mathcal{J}_{m,n} = \{(j,q) \mid k_{j,q} \in \mathcal{K}, k_{j,q} \ne k_{m,n}\}$.

A proof for the case $r = 1$ has been provided in our previous work [14, Appendix A]. For $r > 1$, a similar proof can be constructed using the same approach. Due to the page limit, we provide only a sketch of the proof for Theorem 1 as follows.

*Proof:* For the given optimal solution of Problem (19), we assume that there are $(r+1)$ elements whose modulus are strictly smaller than $\frac{1}{N}$. We keep the other $(N-r-1)$ elements unchanged and keep the arguments of the magnitude operator $|\cdot|$ in constraints (19b) and (19c) the same as the values achieved by the given optimal solution. Since the rank of $\tilde{\mathbf{H}}_{m,n}$ is $r$, we have one additional degree of freedom for adjusting the values of the $(r+1)$ elements. Hence, we can always find a new solution of Problem (19), which achieves a larger value of the objective function in (19a) or has at most $r$ elements not satisfying the CM constraint. This completes the proof. ■

Note that Problem (19) is not a convex optimization problem because a convex objective function is maximized. To address this isssue, the objective function is rewritten as $\left|\mathbf{h}_{m,k_{m,n}}^{\mathrm{H}} \bar{\mathbf{A}}_m \mathbf{d}_{m,n}^{(t-1)}\right| = \left|\mathbf{h}_{m,k_{m,n}}^{\mathrm{H}} \mathbf{a}_{m,n} [\mathbf{d}_{m,n}^{(t-1)}]_n + c\right|$ where $c = \sum_{i \le n-1} \mathbf{h}_{m,k_{m,n}}^{\mathrm{H}} \mathbf{a}_{m,i}^{(t)} [\mathbf{d}_{m,n}^{(t-1)}]_i + \sum_{i \ge n+1} \mathbf{h}_{m,k_{m,n}}^{\mathrm{H}} \mathbf{a}_{m,i}^{(t-1)} [\mathbf{d}_{m,n}^{(t-1)}]_i$ is a constant. According to the triangle inequality, we have $\left|\mathbf{h}_{m,k_{m,n}}^{\mathrm{H}} \bar{\mathbf{A}}_m \mathbf{d}_{m,n}^{(t-1)}\right| \le \left|\mathbf{h}_{m,k_{m,n}}^{\mathrm{H}} \mathbf{a}_{m,n} [\mathbf{d}_{m,n}^{(t-1)}]_n\right| + |c|$ where equality holds if and only if $\mathbf{h}_{m,k_{m,n}}^{\mathrm{H}} \mathbf{a}_{m,n} [\mathbf{d}_{m,n}^{(t-1)}]_n$ and $c$ have the same phase. Thus, the objective function in (19a) is replaced by $\Re(\mathbf{h}_{m,k_{m,n}}^{\mathrm{H}} \mathbf{a}_{m,n} [\mathbf{d}_{m,n}^{(t-1)}]_n e^{-j\nu} + c e^{-j\nu})$ where $\Re(\cdot)$ denotes the real part of a complex number and $\nu$ represents the phase of $c$. With this modification, Problem (19) is a convex problem and the optimal solution $\mathbf{a}_{m,n}^{(t)}$ can be obtained by using CVX. After solving Problem (19) for all $\mathbf{a}_{m,n}$, the modulus normalization is performed as follows

$$[\mathbf{A}_m^{(t)}]_{i,n} = \frac{[\mathbf{a}_{m,n}^{(t)}]_i}{\sqrt{N}|[\mathbf{a}_{m,n}^{(t)}]_i|}, \ \forall m, \ n, \ i, \tag{20}$$

*2) Digital BF:* For given $\{\mathbf{A}_m^{(t)}, \mathbf{D}_m^{(t-1)}\}$, we optimize the digital BF matrices by solving the following problem:

$$\max_{\{\mathbf{D}_m\}} \quad \sum_{m \in \mathcal{M}} \sum_{1 \le n \le |\mathcal{K}_m|} R_{m,n} \tag{21a}$$

$$\text{s.t.} \quad \text{(5e), (5f).} \tag{21b}$$

Problem (21) is a non-convex problem because $R_{m,n}$ is not convex with respect to $\{\mathbf{D}_m\}$. We propose to use the following approach to address this problem, which is based on the important relation between the SINR and the minimum mean squared error (MMSE) [16].

If a single-tap equalizer is employed at the users, the mean squared error of user $k_{m,n}$ can be expressed as

$$\begin{aligned} \varepsilon_{m,n} &= \mathbb{E}\left[\left\|c_{m,n} y_{m,n} - s_{m,n}\right\|_2^2\right] \\ &= \left\|c_{m,n} \hat{\mathbf{h}}_{m,k_{m,n}}^{\mathrm{H}} \mathbf{D}_m - \mathbf{e}_n^{\mathrm{T}}\right\|_2^2 \\ &\quad + \sum_{j \ne m} \left\|c_{m,n} \hat{\mathbf{h}}_{j,k_{m,n}}^{\mathrm{H}} \mathbf{D}_j\right\|_2^2 + \left|c_{m,n}\sigma\right|^2, \end{aligned} \tag{22}$$

where $c_{m,n}$ is the equalization coefficient of the single-tap equalizer at user $k_{m,n}$. $\hat{\mathbf{h}}_{j,k_{m,n}} = \mathbf{h}_{j,k_{m,n}} \mathbf{A}_j^{(t)}$ represents the equivalent channel after analog BF. $\mathbf{e}_n \in \mathbb{R}^{N_{\mathrm{RF}} \times 1}$ is a vector with a one as the $n$th element and zeros elsewhere. The MMSE

can be achieved as follows

$$\frac{\partial \varepsilon_{m,n}}{\partial c_{m,n}}\mid_{c^{\circ}_{m,n}}=0 \Rightarrow$$

$$c^{\circ}_{m,n}=\left(\hat{\mathbf{h}}^{\mathrm{H}}_{m,k_{m,n}}\mathbf{d}^{(t-1)}_{m,n}\right)^{*}\left(\left|\hat{\mathbf{h}}^{\mathrm{H}}_{m,k_{m,n}}\mathbf{d}^{(t-1)}_{m,n}\right|^{2}+\xi_{m,n}\right)^{-1}, \tag{23}$$

where $\xi_{m,n}=\sum\limits_{i\neq n}|\hat{\mathbf{h}}^{\mathrm{H}}_{m,k_{m,n}}\mathbf{d}^{(t-1)}_{m,i}|^2+\sum\limits_{j\neq m}\|\hat{\mathbf{h}}^{\mathrm{H}}_{j,k_{m,n}}\mathbf{D}^{(t-1)}_{j}\|^2_2+\sigma^2$. $(\cdot)^*$ denotes the conjugate. Substituting (23) into (22), we can find that the following equation always holds, i.e.,

$$\varepsilon_{m,n}\mid_{c^{\circ}_{m,n}}=\left(1+\gamma_{m,n}\right)^{-1}, \tag{24}$$

Let $\mathbf{C}=[c_{m,n},1\leq m\leq M,1\leq n\leq N_{\mathrm{RF}}]$. Then Problem (21) is equivalent to

$$\min_{\{\mathbf{D}_m\},\mathbf{C}} \quad \sum_{m\in\mathcal{M}}\sum_{1\leq n\leq|\mathcal{K}_m|}\log_2\varepsilon_{m,n} \tag{25a}$$

$$\text{s.t.} \quad \text{(5e)}, \tag{25b}$$

$$\varepsilon_{m,n}\leq 2^{-r_{m,n}}. \tag{25c}$$

Problem (25) is still non-convex. We introduce an auxiliary function $\psi(u_{m,n})=2^{u_{m,n}-1}\varepsilon_{m,n}-u_{m,n}$ which is minimized at the following point

$$u^{\circ}_{m,n}=-\log_2\varepsilon_{m,n}+1, \tag{26}$$

with minimum value $\psi(u^{\circ}_{m,n})=\log_2\varepsilon_{m,n}$.

Let $\mathbf{U}=[u_{m,n},1\leq m\leq M,1\leq n\leq N_{\mathrm{RF}}]$. Then, Problem (25) is equivalent to

$$\min_{\{\mathbf{D}_m\},\mathbf{C},\mathbf{U}} \quad \sum_{m\in\mathcal{M}}\sum_{1\leq n\leq|\mathcal{K}_m|}\left(2^{u_{m,n}-1}\varepsilon_{m,n}-u_{m,n}\right) \tag{27a}$$

$$\text{s.t.} \quad \text{(5e)}, \tag{27b}$$

$$\varepsilon_{m,n}\leq 2^{-r_{m,n}}. \tag{27c}$$

To find a sub-optimal solution of Problem (27), we alternately optimize $\mathbf{C}$, $\mathbf{U}$, and $\{\mathbf{D}_m\}$ in the course of the iterations. For given $\{\mathbf{A}^{(t)}_m,\mathbf{D}^{(t-1)}_m\}$, we obtain the optimal $\mathbf{C}^{(t)}$ according to (23). For given $\mathbf{C}^{(t)}$, we obtain the optimal $\mathbf{U}^{(t)}$ according to (26). For given $\{\mathbf{A}^{(t)}_m\}$, $\mathbf{C}^{(t)}$, and $\mathbf{U}^{(t)}$, Problem (27) is a convex problem with respected to $\{\mathbf{D}_m\}$ and the optimal $\{\mathbf{D}^{(t)}_m\}$ can be obtained by using CVX.

The overall algorithm for solving Problem (17) is summarized in Algorithm 2.

**Algorithm 2:** Hybrid BF

1: Initialize $\{\mathbf{A}^{(0)}_m,\mathbf{D}^{(0)}_m\}$ according to (18). Let $t=1$.
2: **repeat**
3: Update $\{\mathbf{a}^{(t)}_{m,n}\}$ by solving (19) for given $\{\mathbf{A}^{(t-1)}_m,\mathbf{D}^{(t-1)}_m\}$.
4: Normalization of analog BF matrices according to (20).
5: Update $\mathbf{C}^{(t)}$ according to (23) for given $\{\mathbf{A}^{(t)}_m,\mathbf{D}^{(t-1)}_m\}$.
6: Update $\mathbf{U}^{(t)}$ according to (26) for given $\mathbf{C}^{(t)}$.
7: Update $\{\mathbf{D}^{(t)}_m\}$ by solving (27) for given $\{\mathbf{A}^{(t)}_m\}$, $\mathbf{C}^{(t)}$, and $\mathbf{U}^{(t)}$.
8: Update $t\leftarrow t+1$.
9: **until** Increase of the objective value is below a threshold $\epsilon_2$

Hereto, we find a sub-optimal solution for the UAV-BS positioning, user assignment, and hybrid BF for the considered multi-UAV-BS aided mmWave massive MIMO network. The joint UAV-BS positioning and user assignment problem is first solved by utilizing Algorithm 1 under the assumption of ideal BF. The hybrid BF problem is then solved by utilizing Algorithm 2 under the given positions of UAV-BSs and user assignment. Note that the proposed solution is a centralized strategy, which can be realized by centralizing the computation on a control UAV or a macro-BS on the ground.

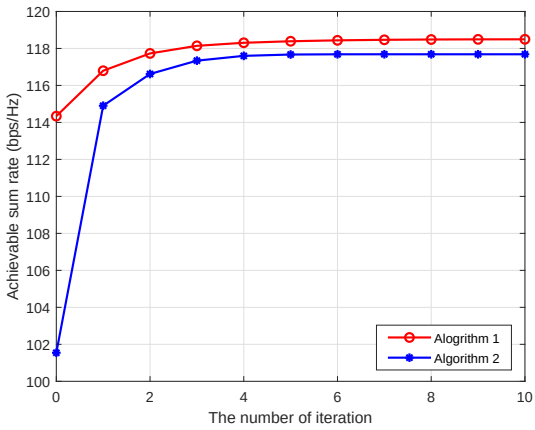


Fig. 2. Convergence of the two proposed algorithms for $P=20$ dBm and $N=16\times16$.

In Algorithm 1, the computational complexities of lines 1 and 3-5 are proportional to $L_0K$ and $L_1K^2$, respectively. $L_0$ and $L_1$ are the maximum numbers of iterations of the K-means initialization and the swap matching, respectively. In Algorithm 2, the maximal complexities of calculating the analog and digital BF matrices for each iteration are $\mathcal{O}(KN^{3.5})$ and $\mathcal{O}(N^7_{\mathrm{RF}})$, respectively. Denote the maximum numbers of iterations of Algorithms 1 and 2 as $T_1$ and $T_2$, respectively. The overall computational complexity of the proposed algorithms is $\mathcal{O}(L_0K+T_1L_1K^2+T_2(KN^{3.5}+N^7_{\mathrm{RF}}))$.

## IV. Performance Evaluation

In this section, we provide simulation results to evaluate the performance of the proposed algorithms. There are $K=12$ users uniformly distributed in a $1\times1$ km$^2$ region. $M=3$ UAV-BSs are deployed at a fixed flight altitude of $H=150$ m. The number of RF chains for each UAV-BS is $N_{\mathrm{RF}}=4$. The carrier frequency is $f_c=38$ GHz and the large-scale path loss exponent is $\alpha=2.3$. The average power of the white Gaussian noise is $\sigma^2=-110$ dBm. The termination thresholds of Algorithms 1 and 2 are set to $\epsilon_1=\epsilon_2=0.05$ bps/Hz. The initial radius of the spherical neighborhood in (14c) is set to $d^{(0)}=100$ m. The step sizes are set to $\kappa_1=1.4$ and $\kappa_2=2$.

Fig. 2 illustrates the convergence of the two proposed algorithms for $P=20$ dBm and $N=16\times16$. As can be observed, both proposed algorithms converge after 5 iterations. The performance gap between the upper bound for the ASR obtained with Algorithm 1 (i.e., the summation of $\bar{R}_{m,n}$ in (7)) and the practical ASR obtained with Algorithm 2 (i.e., the summation of $R_{m,n}$ in (4)) is very small. These results demonstrate that the optimization of the UAV-BS positioning and user assignment under the assumption of ideal BF is reasonable, and the proposed hybrid BF strategy can effectively approach the performance of ideal BF.

Fig. 3 compares the ASR performance of different methods as a function of the transmit power at the UAV-BSs for $N=16\times16$. Three benchmark schemes are considered, namely a fully digital MIMO system with zero-forcing based digital BF,

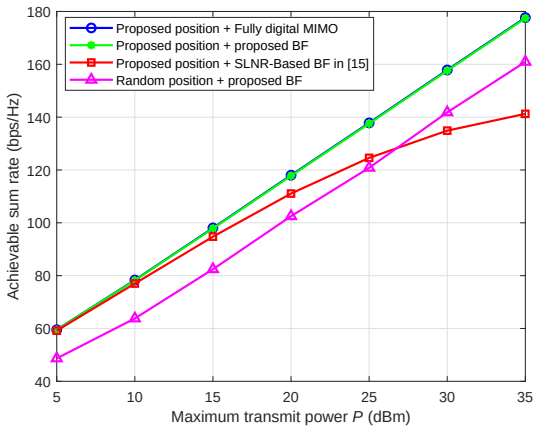


Fig. 3. ASRs of different methods versus transmit powers at the UAV-BSs for $N = 16 \times 16$.

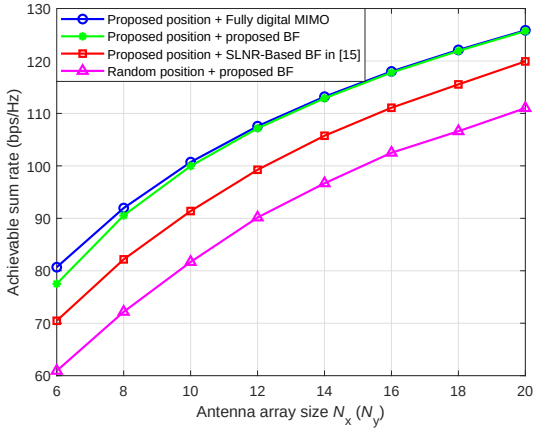


Fig. 4. ASRs of different methods versus antenna array sizes at the UAV-BSs for $P = 20$ dBm.

the signal-to-leakage-plus-noise ratio (SLNR) based hybrid BF scheme proposed in [15], and random UAV-BS positioning, respectively. For all benchmark schemes, the proposed user assignment strategy is employed. As can be observed, the proposed solution achieves an ASR performance very close to the system with fully digital MIMO, and outperforms the other two benchmark schemes. The results in Fig. 3 demonstrate that the proposed hybrid BF method can achieve a near-upper-bound performance. Especially for larger transmit powers, the performance gain of the proposed hybrid BF scheme compared to SLNR based hybrid BF becomes significant.

Fig. 4 compares the ASR performance of different methods as a function of the antenna array size at the UAV-BSs for $P = 20$ dBm. We observe again that the proposed solution closely approaches the upper-bound provided by the fully digital MIMO system and outperforms both the SLNR based hybrid BF and the random UAV-BS positioning schemes. As the antenna array size increases, the performance gap between the proposed hybrid BF scheme and the fully digital MIMO scheme decreases because more degrees of freedom are available for the analog BF matrices to mitigate the interference.

## V. Conclusion

In this paper, we proposed to deploy multiple UAV-BSs to improve the capacity of mmWave massive MIMO networks, where the UAV-BS positioning, user assignment, and hybrid analog-digital BF were jointly optimized for maximization of the ASR, subject to a minimum rate constraint for each user. To solve this severely non-convex problem, we first developed an iterative algorithm which optimizes the UAV-BS positioning and user assignment for maximization of an upper bound on the ASR, under the assumption of ideal BF. Then, we alternately optimized the analog and digital BF matrices for the given UAV-BS positioning and user assignment. Simulation results demonstrated that the proposed solution for multi-UAV-BS aided mmWave networks closely approaches the performance upper bound provided by fully digital MIMO and outperforms two other benchmark schemes.

## Acknowledgement

This work was supported in part by the National Key Research and Development Program (Grant Nos. 2016YFB1200100), and the National Natural Science Foundation of China (NSFC) (Grant Nos. 61827901 and 91738301)

## References

[1] Y. Zeng, Q. Wu, and R. Zhang, "Accessing from the sky: A tutorial on UAV communications for 5G and beyond," *Proc. IEEE*, vol. 107, no. 12, pp. 2327–2375, Dec. 2019.

[2] M. Alzenad, A. El-Keyi, and H. Yanikomeroglu, "3-D placement of an unmanned aerial vehicle base station for maximum coverage of users with different QoS requirements," *IEEE Wireless Commun. Lett.*, vol. 7, no. 1, pp. 38–41, Feb. 2018.

[3] J. Lyu, Y. Zeng, R. Zhang, and T. J. Lim, "Placement optimization of UAV-mounted mobile base stations," *IEEE Commun. Lett.*, vol. 21, no. 3, pp. 604–607, Mar. 2017.

[4] Q. Wu, Y. Zeng, and R. Zhang, "Joint trajectory and communication design for multi-UAV enabled wireless networks," *IEEE Trans. Wireless Commun.*, vol. 17, no. 3, pp. 2109–2121, Mar. 2018.

[5] Y. Sun *et al.*, "Optimal 3D-trajectory design and resource allocation for solar-powered UAV communication systems," *IEEE Trans. Commun.*, vol. 67, no. 6, pp. 4281–4298, Jun. 2019.

[6] D. Xu, Y. Sun, D. W. K. Ng, and R. Schober, "Multiuser MISO UAV communications in uncertain environments with no-fly zones: Robust trajectory and resource allocation design," *IEEE Trans. Commun.*, vol. 68, no. 5, pp. 3153–3172, May 2020.

[7] Z. Xiao, P. Xia, and X.-G. Xia, "Enabling UAV cellular with millimeter-wave communication: potentials and approaches," *IEEE Commun. Mag.*, vol. 54, no. 5, pp. 66–73, May 2016.

[8] C. Zhang, W. Zhang, W. Wang, L. Yang, and W. Zhang, "Research challenges and opportunities of UAV millimeter-wave communications," *IEEE Wireless Commun.*, vol. 26, no. 1, pp. 58–62, Feb. 2019.

[9] L. Yang and W. Zhang, "Beam tracking and optimization for UAV communications," *IEEE Trans. Wireless Commun.*, vol. 18, no. 11, pp. 5367–5379, Nov. 2019.

[10] J. Zhao, F. Gao, Q. Wu, S. Jin, Y. Wu, and W. Jia, "Beam tracking for UAV mounted SatCom on-the-move with massive antenna array," *IEEE J. Select. Areas Commun.*, vol. 36, no. 2, pp. 363–375, Feb. 2018.

[11] J. Zhang, W. Xu, H. Gao, M. Pan, Z. Feng, and Z. Han, "Position-attitude prediction based beam tracking for UAV mmWave communications," in *Proc. IEEE Int. Conf. Commun.*, May 2019.

[12] Z. Feng, L. Ji, Q. Zhang, and W. Li, "Spectrum management for mmwave enabled UAV swarm networks: Challenges and opportunities," *IEEE Commun. Mag.*, vol. 57, no. 1, pp. 146–153, Jan. 2019.

[13] Z. Xiao *et al.*, "Unmanned aerial vehicle base station (UAV-BS) deployment with millimeter-wave beamforming," *IEEE Internet Things J.*, vol. 7, no. 2, pp. 1336–1349, Feb. 2020.

[14] L. Zhu, J. Zhang, Z. Xiao, X. Cao, X.-G. Xia, and R. Schober, "Millimeter-wave full-duplex UAV relay: Joint positioning, beamforming, and power control," *IEEE J. Sel. Areas Commun.*, 2020 (To appear).

[15] S. Sun, T. S. Rappaport, and M. Shaft, "Hybrid beamforming for 5G millimeter-wave multi-cell networks," in *Proc. IEEE Conf. Comput. Commun. Workshops*, Apr. 2018, pp. 589–596.

[16] W. Xu *et al.*, "Robust beamforming with partial channel state information for energy efficient networks," *IEEE J. Sel. Areas Commun.*, vol. 33, no. 12, pp. 2920–2935, Dec. 2015.